Contents lists available at ScienceDirect

Journal of Theoretical Biology

journal homepage: www.elsevier.com/locate/vitbi



How the resource supply distribution structures competitive communities



Ravi Ranjan a,b,c,d,e,*, Christopher A, Klausmeier c,d,e,f

- ^a Helmholtz Institute of Functional Marine Biodiversity at the University of Oldenburg (HIFMB), Ammerländer Heerstraße 231, D-26129 Oldenburg, Germany
- ^b Alfred-Wegener-Institute, Helmholtz-Centre for Polar and Marine Research (AWI), Am Handelshafen 12, 27570 Bremerhaven, Germany
- ^c W. K. Kellogg Biological Station, Michigan State University, 3700 E. Gull Lake Dr, Hickory Corners, MI 49060, USA
- ^d Department of Plant Biology, Michigan State University, 612 Wilson Road, East Lansing, MI 48824, USA
- ^e Ecology, Evolution, and Behavior Program, Michigan State University, 293 Farm Lane, East Lansing, MI 48824, USA
- Department of Integrative Biology, Michigan State University, Natural Science Building, 288 Farm Lane, East Lansing, MI 48824, USA

ARTICLE INFO

Article history: Received 23 August 2021 Revised 1 February 2022 Accepted 4 February 2022 Available online 7 February 2022

Keywords: Competition Adaptive dynamics Trait patterns Eco-evolutionary dynamics

ABSTRACT

Competition is a pervasive interaction known to structure ecological communities. The Lotka-Volterra (LV) model has been foundational for our understanding of competition, and trait-based LV models have been used to model community assembly and eco-evolutionary phenomena like diversification. The intrinsic growth rate function is determined by the underlying resource distribution and is a key determinant of the resulting diversity, traits and abundances of species. In these models, the width of the resource distribution relative to the width of the competition kernel has been identified as a key parameter that leads to diversification. However, studies have only investigated the impact of width at just a few discrete values, while also often assuming the intrinsic growth rate function to be unimodal. Thus, the impact of the underlying resource distribution's width and shape together remains incompletely explored, particularly for large, diverse communities. In this study, we vary its width continuously for two shapes (unimodal and bimodal) to explore its impact on community structure. When the resource distribution is very narrow in both the unimodal bimodal cases, competition is strong, leading to exclusion of all but the best-adapted species. Wider resource distributions allow stable coexistence, where the traits of the species depend on the shape of the resource distribution. Extremely wide resource distributions support a diverse community, where the strength of competition ultimately determines the diversity and traits of coexisting species, but their abundances reflect the underlying resource distribution. Further, competition acts to maximize the use of available resources among the competing species. For large communities, the shape of resource distribution becomes immaterial and the width determines the diversity. These results affirm and extend our understanding of limiting similarity.

© 2022 Elsevier Ltd. All rights reserved.

1. Introduction

Competition structures communities and is ubiquitous in nature (Connell, 1983; Elton, 1946). The Lotka-Volterra (LV) competition model is a phenomenological model that underlies much of our understanding of competition (Lotka, 1925; Volterra, 1926), particularly the two-species LV model. However, the application of these models to natural communities that can have tens or hundreds of species in competition is not straightforward. Because each pair of species requires a pair of competition coefficients apart

E-mail address: ravi.ranjan@hifmb.de (R. Ranjan).

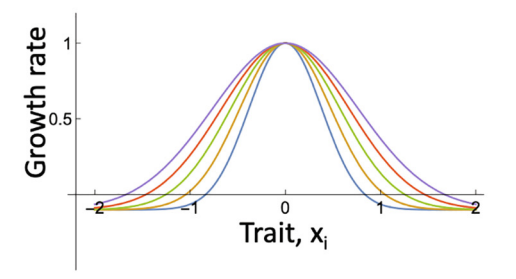
from their own growth rates, the number of parameters in the LV model increases quadratically with the number of species, making parameterization and complete exploration impossible.

To address this enormous complexity in parameterization, one approach is to explicitly ground the parameters in species traits, thus making the model more mechanistic. Focusing on species traits has several advantages (McGill et al., 2006; Messier et al., 2010). Both ecological processes such as competition and evolutionary processes such as natural selection act on species through their traits. Traits offer a natural currency to make comparisons between disparate communities. Therefore, focusing on traits instead of species identities allows us a biologically significant way to cut through the complexity of diverse communities, allowing us to extract meaningful insights (e.g. in Hui et al., 2018).

^{*} Corresponding author at: Helmholtz Institute for Functional Marine Biodiversity at the University of Oldenburg (HIFMB), Ammerländer Heerstr. 231, 26129 Oldenburg, Germany,

a) Unimodal growth rate function

b) Bimodal growth rate function



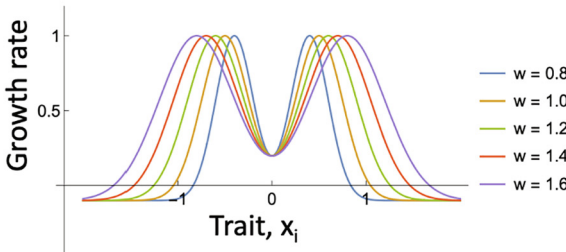


Fig. 1. The two intrinsic growth rate functions plotted at different values of *w*, the width parameter. A) The unimodal function represents a resource distribution where there is one prominent resource in the environment. B) The bimodal function represents a different environment where there are two prominent resources.

Trait-based LV models can be derived from more-mechanistic consumer-resource models (Ackermann and Doebeli, 2004; MacArthur, 1972), and have frequently been used to understand the interplay of competition and evolution (Barabás et al., 2012; Fort et al., 2009; Polechová and Barton, 2005; Roughgarden, 1979; Scheffer and van Nes, 2006). The width and shape of the resource distribution has been shown to play an important role in determining the diversity of communities. A broad consensus has emerged from previous work that the width of the resource distribution determines community diversity (Barabás et al., 2016; Barabás and Meszéna, 2009; Kremer et al., 2017; Szabó and Meszéna, 2006). Wider resource distributions result in wider trait ranges where intrinsic growth rate of species is positive, also known as the fundamental community (Klausmeier et al., 2020). Simply put, wider fundamental communities have more room in which to pack species, resulting in more diverse communities.

While studies have investigated the impact of width and shape on various aspects of the diversification process, they each have some limitations. First, most studies have assumed unimodal carrying capacity functions (quadratic or Gaussian). Kisdi also considered monotonic functions (linear and convex) (Kisdi, 1999); Barabas and D'Andrea also considered triangular (Barabás et al., 2016); and Szabo & Meszena also considered rectangular and fractal (Szabó and Meszéna, 2006). Yet, as far as we know, none have considered bimodal carrying capacity functions. Second, most studies using the LV model to study diversification typically focus on the transition from one species to two (Dieckmann and Doebeli, 1999). Those that consider more species-rich communities use either a few discrete width-values (Barabás et al., 2016; Pastore et al., 2021; Szabó and Meszéna, 2006) and/or focus on evolutionary divergence through time (Birand and Barany, 2014; Bonsall et al., 2004; Cressman et al., 2017; Pontarp et al., 2015). Therefore, the impact of continuously varying the width of resource distributions with different shapes on the generation of large numbers of species and their traits has not been investigated (although see (Barabás et al., 2016; Landi et al., 2013; Szabó and Meszéna, 2006)).

To address this gap, we investigate a trait-based LV model across a range of resource distribution widths and with two resource-distribution shapes. Keeping with previous studies, we assume a Gaussian competition kernel. For the resource distribution, we choose a traditional unimodal function as well as a more novel bimodal function. For each of the shapes of the intrinsic growth rate function, we solve for the Evolutionarily Stable Community (ESC) (Edwards et al., 2018; Kremer et al., 2017) as a function of the width of the resource distribution. We find that wider resource distributions result in higher diversity in the community. At low widths of the resource distribution, the bimodal distribution results in twice as many species as the unimodal, but not for very high widths. For very high widths, we see the same diversity regardless of the shape of the resource distribution function. We

also find that Matessi and Jayakar's maximization principle (Matessi and Jayakar, 1980, 1981) (an extension of MacArthur's purely ecological minimization principle (MacArthur, 1970, Mac Arthur, 1969) to co-evolving species) is applicable to our model, with multiple species at various widths of the intrinsic growth rate function.

2. Model

2.1. Model formulation

We model competition using a trait-based LV model, where the number of species \mathcal{N} is not fixed *a priori* but allowed to emerge via community assembly and eco-evolutionary processes. Each species i has population density n_i , trait value x_i , and per-capita growth rate

$$\frac{1}{n_i}\frac{dn_i}{dt} = r(x_i) - \sum_{i=1}^{N} \alpha(x_i, x_j) n_j = g(x_i; \overrightarrow{n}, \overrightarrow{x})$$
 (1)

A species' trait value x_i determines its intrinsic growth rate $r(x_i)$, the growth rate when no competitors are present. The intrinsic growth rate function implicitly models its consumption of resources (Ackermann and Doebeli, 2004; MacArthur and Levins, 1967) and thus captures the resource supply distribution. Since this distribution might differ between sites, a range of different intrinsic growth rate functions are possible depending upon the environment. The competition coefficient $\alpha(x_i, x_i)$ determines the strength of competition between species i and j, and depends on the difference between their traits x_i and x_j . Further, we assume that the strength of intraspecific competition is 1 ($\alpha(x_i, x_i) = 1$), so that the equilibrium density of the species by itself (carrying capacity) equals its fundamental growth rate $r(x_i)$. More generally, the per-capita growth rate is denoted by the function $g(x_i; \overrightarrow{n}, \overrightarrow{x})$, to signal its dependence on the trait x_i of the focal species i and the whole community's abundances (\overrightarrow{n}) and traits (\overrightarrow{x}) . Since the traits determine the species' abundances at an ecological equilibrium, we simplify the invader growth rate as $g(x_i; \vec{x})$ at equilibrium. This simplification only applies at equilibrium since the invader's growth rate does depend on the densities of the resident species when the resident community is not at equilibrium. Note that our formulation of the LV model in Eq. (1) differs from the more common formulation that uses the carrying capacity as the traitdependent term. We believe that this formulation is more intuitive because it separates the per capita growth rate of a species into two terms - the density-independent intrinsic growth rate and

the density-dependent effect of competition — and is better behaved outside a species' fundamental niche, when $r(x_i) < 0$ (Kuno, 1991; Mallet, 2012).

It is important to note that while our model is phenomenological in nature, LV models can be mapped on to consumer-resource models (MacArthur, 1972; MacArthur and Levins, 1967) under a restrictive set of assumptions. Specifically, when either the resource carrying capacity (resource density when no consumers are present) or the consumer mortality are dependent on the consumer trait, mechanistic consumer-resource models can be converted to a LV form like ours with symmetric competition coefficients and trait-dependent intrinsic growth rate (Section 2 in the Supplementary information to Pastore et al., 2021). However, when both the resource carrying capacity and the consumer mortality are constants, a LV model with symmetric competition and trait-dependent intrinsic growth rate cannot be derived from a mechanistic consumer-resource model (Appendix 1 in Ackermann and Doebeli, 2004). Therefore, our LV model captures the essence of resource competition while incorporating biological realism through trait-dependent intrinsic growth rates.

2.2. Functional forms

To represent different resource distributions, we use two growth rate functions. The first is a displaced unimodal Gaussian function, for which a single trait ($x_i = 0$, in this case) yields the maximum intrinsic growth rate (Fig. 1a). The intrinsic growth rate is given by:

$$r(x_i) = k_1 \left(\exp\left(-\frac{\left(\frac{x}{wk_3}\right)^2}{2\sigma_e^2}\right) \right) - k_2$$
 (2)

The parameter w determines the half-width of the intrinsic growth rate function. Note that the intrinsic growth rate can be negative as we assume that the environment only allows species with a range of traits to grow. Constants $k_1 = 1.1$ and $k_2 = 0.1$ determine the intrinsic growth rate at the peak and ensure that it is negative at very high and very low trait values.

The second growth rate function is bimodal, which has two trait values that allow for a maximum intrinsic growth rate (Fig. 1b).

$$r(x_i) = k_1 \left(\exp\left(-\frac{\left(\frac{x}{wk_3} - 0.5\right)^2}{2\sigma_e^2}\right) + \exp\left(-\frac{\left(\frac{x}{wk_3} + 0.5\right)^2}{2\sigma_e^2}\right) - k_4$$
 (3)

The constants $k_1=1.1$ and $k_4=0.10037$ ensure that the intrinsic growth rate matches the unimodal function (2) at the peaks. For both unimodal and bimodal functions, σ_e determines the width of the peaks. In the bimodal case, σ_e also determines the intrinsic growth rate in the average environment ($x_i=0$) since it controls the width of each of the two peaks. For the purposes of this study, we fix this width at $\sigma_e=0.25$ so that the intrinsic growth rate at $x_i=0$ in the bimodal case is positive. In both cases, the constant $k_3=1.04575$ ensures that the region of trait space where $r(x_i)>0$ for the bimodal function is the same as the unimodal one (2) at any w. The rest of the parameters are the same as in the unimodal case.

The competition coefficient is determined by the competition kernel, which we take to be a Gaussian function:

$$\alpha(x_i, x_j) = \exp\left(-\frac{(x_i - x_j)^2}{2}\right) \tag{4}$$

Here, x_i and x_j are the traits of the competing consumers i and j and the competition strength between them decreases with increasing magnitude of trait difference. Species with similar traits, therefore,

are stronger competitors as opposed to species with dissimilar traits. Note that this function implies that the strength of competition is symmetric (see Gallien et al., 2018 for similar work on the asymmetric case).

2.3. Model analysis

We focus here on the endpoint of the eco-evolutionary community assembly process, where invasion is impossible and directional selection stops, called an Evolutionarily Stable Community (Edwards et al., 2018; Klausmeier et al., 2020; Kremer et al., 2017; Minoarivelo and Hui, 2016). In contrast to adaptive dynamics (Geritz et al., 1998), we do not restrict the phenotypes of potential invaders to be similar to resident species (Brown and Vincent, 1987). This could model either large mutations of residents, or immigration of distinct species from the regional species pool (community assembly). Therefore we focus on global evolutionary stability, which prevents the system from getting stuck on a local but not global ESS (Geritz et al., 1999). In most cases, the same equilibrium arises in both the ESC and adaptive dynamics frameworks (Klausmeier et al., 2020). We briefly point out situations where it does not below.

One approach to determining the Evolutionarily Stable Community (ESC) is to apply an invasion-based algorithm to build up the ESC for a fixed value of the parameter w. In an empty environment, we start with a single invader species with trait x_1 invading an empty environment. Since there are no competitors, the invasion growth rate $(\frac{1}{n_1} \frac{dn_1}{dt})$ for the first invader is $r(x_1)$ and invasion is only successful if x_1 is such that $\frac{1}{n_1} \frac{dn_1}{dt} = r(x_1) > 0$.

After a successful invasion, the former invader becomes a resident, and we solve for its equilibrium abundance \widehat{n}_1 by setting $g(x_1;x_1)=0$. We then introduce a new invader with trait value x_0 at low abundance and calculate its invasion fitness (per-capita growth rate). With a single species as resident (x_1) , the invasion fitness of the invader is:

$$\frac{1}{n_0} \frac{dn_0}{dt} = g(x_0; x_1) = r(x_0) - \alpha(x_0, x_1) \hat{n}_1 \tag{5}$$

As before, invasion succeeds if $g(x_0;x_1)>0$ and fails if $g(x_0;x_1)<0$. The outcome of a successful invasion further depends on the outcome of the reverse invasion $(x_1 \text{ invades } x_0)$, which is determined by the sign of $g(x_1;x_0)$. If $g(x_1;x_0)<0$, we assume that the invader replaces the resident, otherwise the two coexist (this is not necessarily the case for non-local invaders, where unprotected coexistence is possible (Dercole and Geritz, 2016; Priklopil, 2012), but such coexistence is not robust to stochasticity and we never encountered it in our model). More generally, we denote a community of $\mathscr N$ residents as $\overrightarrow x$ and the fitness of an invader x_0 invading a community with residents $\overrightarrow x$ is $g(x_0; \overrightarrow x)$:

$$g\left(x_0; \overrightarrow{x}\right) = r(x_0) - \sum_{i=1}^{N} \alpha(x_0, x_i) \widehat{n}_i$$
 (6)

The fitness gradient, $\frac{\partial g}{\partial x_0}\Big|_{x_0=x_i}$ determines the direction and strength of directional selection on species i, which continues until an *evolutionary equilibrium* is reached ($\frac{\partial g}{\partial x_0}=0$ for all species i). If an evolutionary equilibrium is stable such that no other strategy can invade it, it is called *evolutionary stable strategy (ESS)*. Evolutionary stability is typically measured locally, using the second derivative of invasion fitness with respect to the trait of the invader ($\frac{\partial^2 g}{\partial x_0^2}$). If $\frac{\partial^2 g}{\partial x_0^2} < 0$ at an evolutionary equilibrium, the equilibrium is locally evolutionarily stable. However, $\frac{\partial^2 g}{\partial x_0^2} > 0$ means that the equilibrium is at a fitness minimum and is called a *branching point* when it is convergence stable (however see Dercole et al., 2016 for caveats).

In adaptive dynamics *sensu stricto*, the invaders are considered to be mutants of resident species, with small mutations (Della Rossa et al., 2015; Dercole et al., 2016; Geritz et al., 1998; Metz et al., 1996). Thus, the invaders are limited to nearby trait values of the resident. In that case, a local ESS is the endpoint of the assembly process, since local evolutionary stability of the evolutionary equilibrium is enough to prevent further invasions from occurring. However, to account for invaders with substantially different traits from the residents (either large mutations or immigration of other species), we look for globally evolutionarily stable equilibria, which we call *Evolutionary Stable Communities* (Edwards et al., 2018; Kremer et al., 2017).

This eco-evolutionary community assembly algorithm is wellestablished (Edwards et al., 2018; Klausmeier et al., 2020; Kremer et al., 2017), but can be computationally inefficient, particularly for diverse communities. Because we are interested in how the width of the resource distribution (w) determines the ESC. we instead use a more efficient approach to generate bifurcation diagrams using continuation as follows (see also Klausmeier et al., 2020; Landi et al., 2013). First, we calculate the evolutionary equilibrium of a single species ($\mathcal{N}=1$), at a narrow width of the resource distribution to ensure evolutionary stability, using Newton's method to numerically solve for equilibrium abundance (\widehat{n}_1) and trait value (\widehat{x}_1) by setting $g(\widehat{x}_1;\widehat{x}_1)=0$ and $\frac{\partial g}{\partial x_0}\Big|_{x_0=\widehat{x}_1}=0$. Then we increase w by a small amount δw , extrapolating the previous evolutionary equilibrium as an initial guess for Newton's method to solve for the evolutionary equilibrium at $w_0 + \delta w$. Using the previous equilibrium as an initial guess helps to ensure convergence and saves computational time, particularly when the number of species is high, thus allowing us to track the ESC effectively as w changes. At each value of w, we check local $(\partial^2 g/\partial x^2 < 0)$ and global evolutionary stability $(\max g(x_0; \overrightarrow{x}))$ < 0) and verify that no species have gone extinct ($\hat{n}_i > 0$ for all i), which never occurred in our model. We also check for dynamic stability (both ecological and convergence stability) by calculating eigenvalues of the Jacobian matrix of the coupled population equations (Eq. (1)) and trait equations $dx_i/dt = \frac{\partial g}{\partial x_0}\Big|_{x_0=x_i}$; the ESC was always convergence stable and ecologically stable (for a discussion on non-stationary coexistence, see Landi et al., 2013). If the community loses evolutionary stability at one of these steps, a bifurcation occurs. In this case, we add another species to the community by adding $g(x_{\mathcal{N}+1})=0$ and $\frac{\partial g}{\partial x_0}\Big|_{x_0=x_{\mathcal{N}+1}}=0$ to the set of equations and solve for the equilibrium abundances and traits of the new ESC at a w value just past the bifurcation point. This solution serves as a new set of initial guesses for an ESC with $\mathcal{N}+1$ species, allowing us to continue varying w and solving for ESCs.

We used the EcoEvo package (Klausmeier, 2020) in Wolfram Mathematica 12 (Wolfram Research, Inc., 2021) to do the numerical analyses for the bifurcation diagram. The resulting bifurcation diagrams allow us to contrast the diversification patterns for large communities under two different shapes of the resource distribution and investigate the role of the resource distribution vs. competition in structuring these communities.

3. Results

For each intrinsic growth function, we analyze how the Evolutionarily Stable Communities (ESCs) depend on the width of the growth function. We start with the smallest ESCs in both cases – one species for the unimodal growth function and two for the bimodal growth function. Increasing the width of the growth function leads to diversification via evolutionary bifurcations. We

illustrate the initial bifurcations using invasion fitness landscapes. Since these bifurcations repeat to generate diverse communities, we then analyze the trait patterns in large communities generated under each intrinsic growth function. Finally, we investigate the impact of the intrinsic growth rate functions on the ESCs by comparing the resulting trait patterns in the respective bifurcation plots.

3.1. Unimodal intrinsic growth function

3.1.1. Initial bifurcations

To begin, we examine in detail the initial bifurcations, from one to two, and two to three species. Low values of w represent a narrow resource distribution, so that species compete strongly with each other. In the narrowest environments, there is no room for niche differentiation, so that the species with the highest intrinsic growth rate excludes all others. The evolutionary equilibrium $\hat{x}_1 = 0$ is both convergence and evolutionarily stable (Fig. 2a; Geritz et al, 1998).

Increasing the width of the resource distribution, w, increases the invasion fitness of species with traits dissimilar to $x_i = 0$ (both higher and lower) due to the weakened competition. At the bifurcation point w = 1.5511, the second derivative of invasion fitness becomes zero (Fig. 2b) (Della Rossa et al., 2015; Dercole et al., 2016). Beyond the bifurcation point, the single species ESC becomes unstable (Fig. 2c) resulting in a two-species ESC (Fig. 2d). Notably, this bifurcation occurs through the local evolutionary instability of the single-species ESS, so the new two-species ESC is reachable under adaptive dynamics *sensu stricto*.

As w increases further, the increased width of the resource distribution allows the traits of the two species in the ESC to become more dissimilar to reduce competition. At these ESCs, although an invader with $x_0 = 0$ has the highest intrinsic growth rate, it also experiences strong competition from both the residents, which prevents its invasion (Fig. 2d). As w continues to increase, the increasing dissimilarity between the two species in the ESC weakens competition for an invader with $x_0 = 0$ (Fig. 3a). The invasion fitness of a species with $x_0 = 0$ is zero at the bifurcation point (Fig. 3b). For larger w, it has a positive invasion fitness (Fig. 3c). Invasion of this unstable community results in a new threespecies ESC (Fig. 3d) (for a discussion of the consequences of non-invasion of an empty niche, see Hui et al., 2021, Hui et al., 2016). Interestingly, this eco-evolutionary transcritical bifurcation results from the loss of global stability of the two-species ESC while it remains locally stable. Since adaptive dynamics sensu stricto only allows invaders with small trait differences, the three-species ESC would initially be unreachable under adaptive dynamics, but reachable by large mutation or immigration of other pre-existing species.

3.1.2. Large communities

Having investigated in detail the bifurcations from one to three species at low resource distribution width, we now focus on a larger range of resource-distribution widths that support up to 25 species (Fig. 4). Large widths of the resource distribution support greater diversity, which arises through the two types of bifurcations we characterized in the previous section. As the community goes from an odd to an even number of species, it undergoes a bifurcation where one of the species loses its local evolutionary stability, similar to the transition from one to two species (Fig. 2). As the community goes from an even to an odd number of species, it undergoes a bifurcation where the community loses global evolutionary stability and becomes invasible by the central species with $x_0 = 0$, similar to the transition from two to three species (Fig. 3).

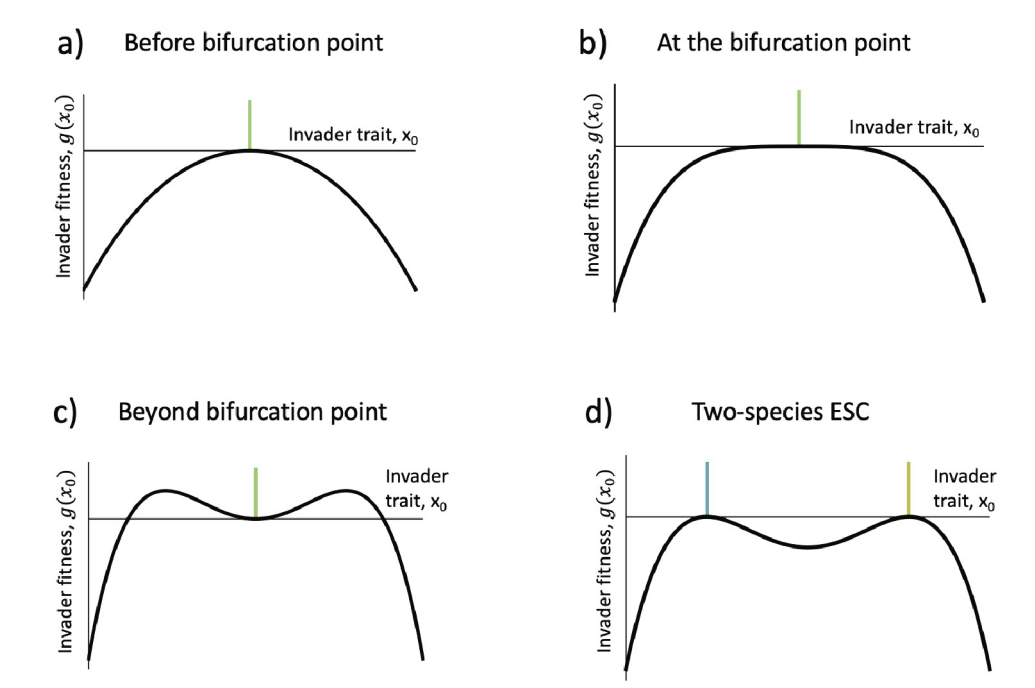


Fig. 2. The invasion fitness landscapes during the transition from one to two species at ESC. The colored vertical bars in the figures represent the traits of the resident species. (a) Before the bifurcation point (w = 1.55), the invasion fitness of an invader with any trait value is negative. (b) At the bifurcation point (w = 1.5511), the invasion fitness of the invaders with traits close to resident species at ESC ($x_i = 0$) is zero. (c) As the width increases beyond the bifurcation point (w = 1.5512), the invasion fitness of the invaders becomes positive and the resident becomes susceptible to invasion. (d) Finally, after invasion at w = 1.5561, a new ESC with two species emerges.

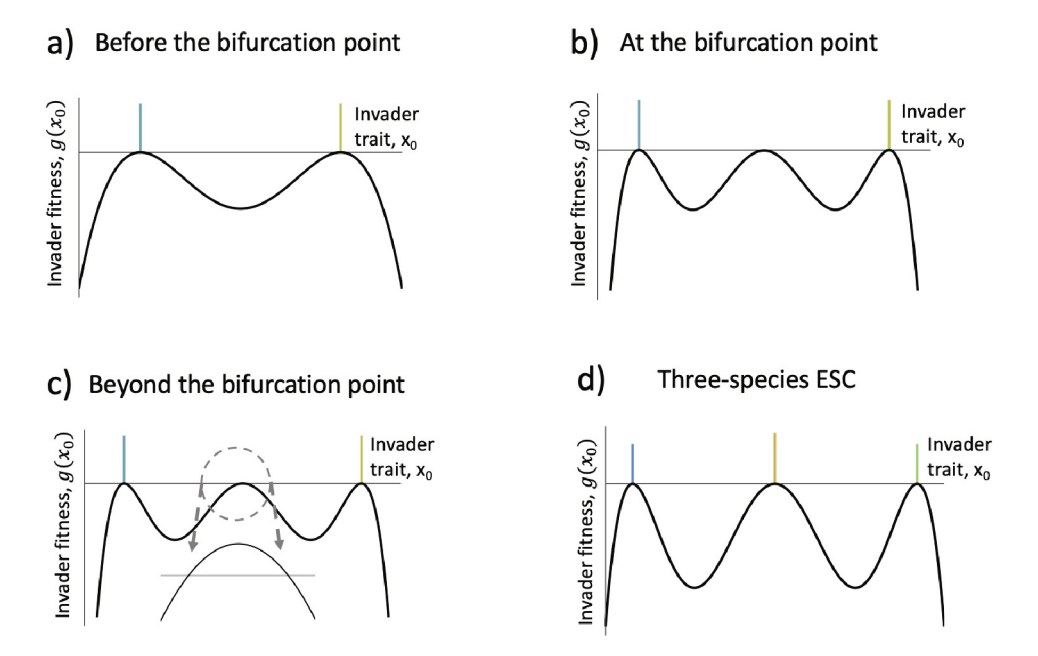


Fig. 3. The invasion fitness landscapes during the transition from two to three species at ESC. The colored vertical bars in the figures represent the traits of the resident species. (a) Before the bifurcation point (w = 1.72939), no invader can invade the two-species ESC. (b) At the bifurcation point (w = 1.82939), the invasion fitness of the invader with trait, $x_i = 0$ is zero. (c) As the width increases beyond the bifurcation point (w = 1.8294), the invader faces weakened competition, and its invasion fitness becomes positive. The inset shows a magnified picture of the invasion fitness landscape. (d) At w = 1.93939, invasion results in a new ESC with three species.

As predicted by classical theory (Abrams, 1983; MacArthur and Levins, 1967), competition results in approximately evenly spaced traits at any width of the resource distribution due to the character displacement between the species (Fig. 4). Interestingly, the role of the shape of the intrinsic growth function is not immediately apparent from the trait patterns in this case, apart from setting the range of species with positive growth (white region of Fig. 4), termed the fundamental community (Klausmeier et al., 2020). The width of the resource distribution determines the species

richness because species divide the available trait space between them, each with a roughly constant distance between species.

3.2. Bimodal intrinsic growth function

3.2.1. Initial bifurcations

A bimodal intrinsic growth rate function such as Eq. (3) is representative of an environment with two prominent resources. At low widths of the resource distribution, each peak behaves like

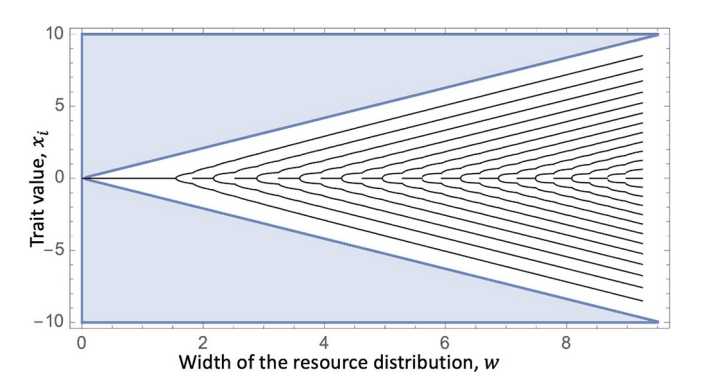


Fig. 4. The trait patterns of communities up to 25 species as the width of the unimodal intrinsic growth function is increased. The shaded portion is outside the fundamental niche, where the intrinsic growth rate of each species is negative. Competition results in roughly equal spacing of the traits within the fundamental niche.

an independent unimodal growth rate function. As in the unimodal case, we first examine the initial bifurcations – going from two to four species, and then from six to seven species. We skip discussion of the bifurcation from four to six species since it is similar to the bifurcation from two to four species.

At low w, only a narrow range of species can invade the empty environment. Typically, in the limit as $w \to 0$, coexistence is impossible and the species with the greatest intrinsic growth rate is a global ESS. However, the growth function in Eq. (3) is atypical, because the growth rate at the two peaks is exactly equal. Therefore, at low w, the ESC consists of the two species with maximum intrinsic growth rate (Fig. 5a).

Increasing the width of the resource distribution increases the dissimilarity between traits that maximize the intrinsic growth rate, which also increases the trait differences between the species in the ESC. Upon further increasing *w*, two bifurcations occur

simultaneously, one corresponding to each peak of the resource distribution. At this bifurcation point, the invasion fitness of the invaders with traits with small differences from the resident appears to be zero (Fig. 5b), apparently similar to the first bifurcation in the unimodal model where the ESC goes from one-species to two species (Fig. 2). However, a close inspection (Fig. 5c) shows that this is actually a nonlocal bifurcation as in Fig. 3, although the nonlocal invader is so close to the resident that the two scenarios are practically indistinguishable. Increasing w results in less competition for potential invaders with traits dissimilar to the species at the peak. As the width crosses the bifurcation point, the evolutionary equilibrium can be invaded (Fig. 5d). Upon invasion, each peak allows for two residents at the new ESC, bringing the overall number of species to four (Fig. 5e).

As w increases further, the same type of bifurcation repeats. resulting in an addition of one species under each peak of the resource distribution, bringing the overall diversity to six species. However, increasing w further leads to a different type of bifurcation, which takes the ESC from six species to seven species (Fig. 6). The increasing width of the intrinsic growth function results in increased distance between the traits that maximize the intrinsic growth rate. Since the species at ESC follow these peaks, they are roughly equally spaced under each peak and become more and more dissimilar as the width of the resource distribution increases (Fig. 6a). At the bifurcation point, the central invader with $x_i = 0$ is on the cusp of invasion and has zero invasion fitness due to reduced competition (Fig. 6b). Increasing the width further results in the loss of global stability for the resident community, and leaves it open to invasion (Fig. 6c). After the invasion by the species with $x_i = 0$, the new resident community with seven species regains global stability and is therefore a new ESC (Fig. 6d). As with the second bifurcation in the unimodal case, this bifurcation constitutes the loss of global stability for the resident and is therefore not reachable through the small mutations assumed by classic adaptive dynamics methods.

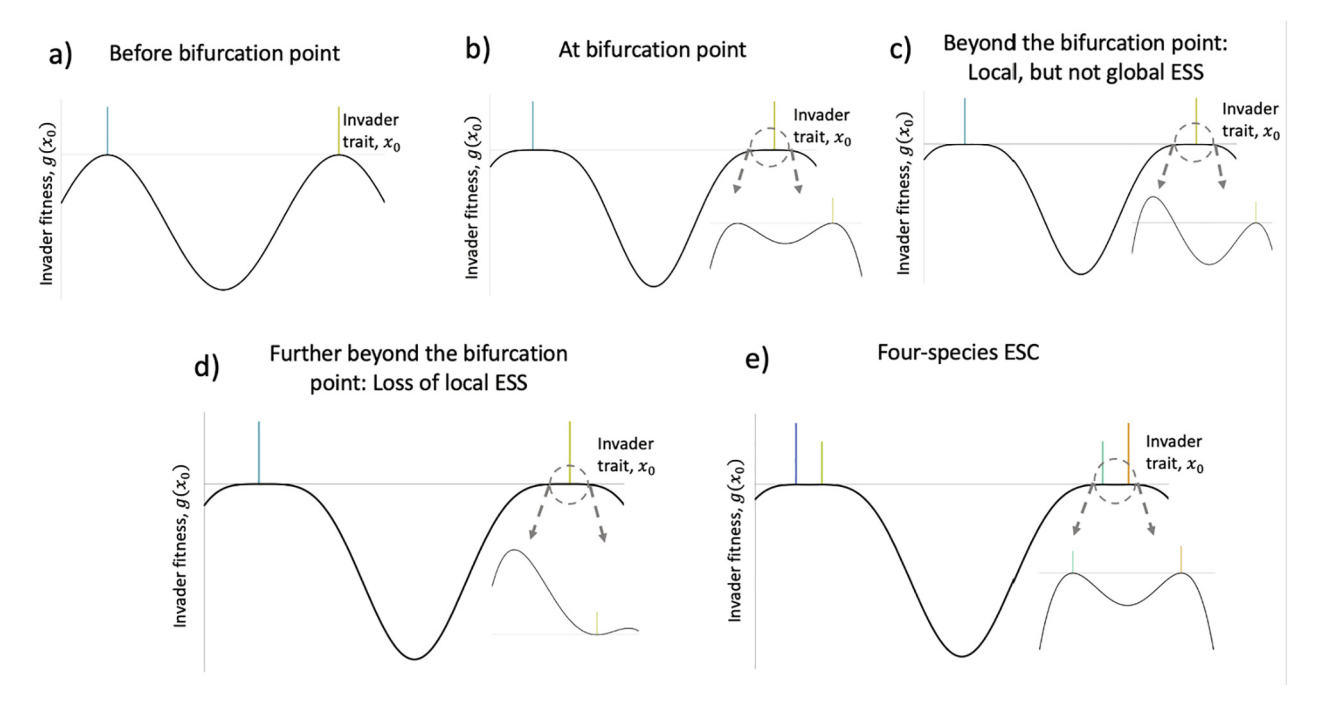


Fig. 5. The invasion fitness landscapes during the transition from two to four species at ESC. The colored vertical bars in the figures represent the traits of the resident species. (a) Before the bifurcation point (w = 2.86283), the ESC consists of two species. (b) At the bifurcation point (w = 2.96283), the invasion fitness of the invaders with traits close to resident species at both peaks is zero. (c) For a very small parameter range (2.962837 < w < 2.963012) after the bifurcation point, the evolutionary equilibrium loses global stability but maintains local stability. (d) As the width further increases (w = 2.96383), the evolutionary equilibrium becomes locally unstable. Thus, the invasion fitness of the invaders at each peak becomes positive (shown in inset) and the resident community can be invaded. (e) After invasion (w = 3.06283), a new ESC with four species emerges. A magnified view of the fitness landscape at each peak is shown in inset.

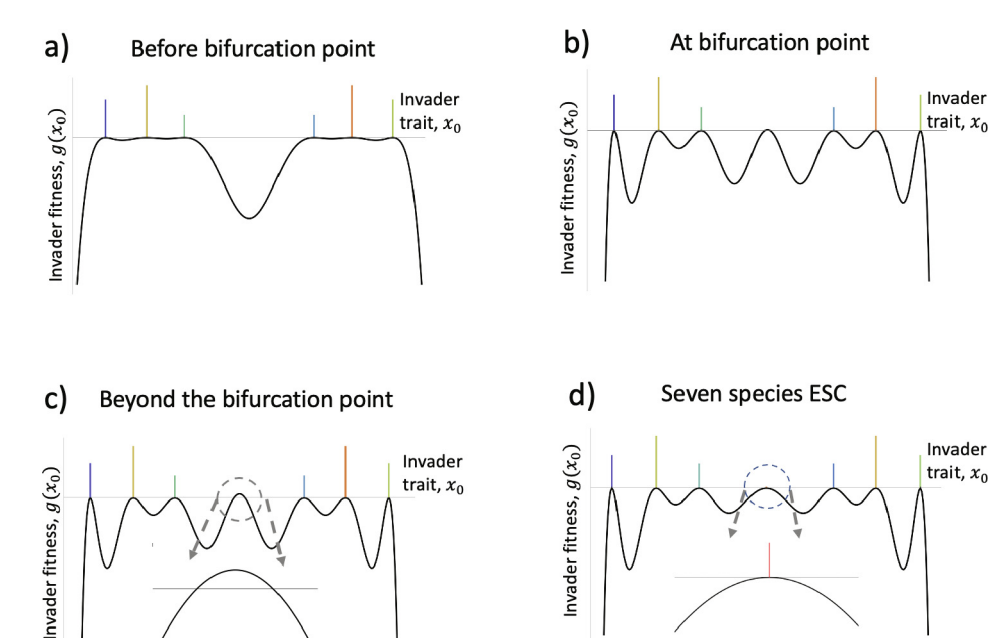


Fig. 6. The invasion fitness landscapes during the transition from six to seven species with a bimodal growth function. The colored vertical bars in the figures represent the traits of the resident species. (a) Before the bifurcation point (w = 3.74248), the ESC consists of six species. (b) At the bifurcation point (w = 3.84248), the invasion fitness of the invader with trait, $x_0 = 0$ is zero. (c) As we cross the bifurcation point (w = 3.84258), the invader $x_0 = 0$ faces weakened competition and its invasion fitness becomes positive (shown in inset). (d) Invasion of the resident community results in a new ESC with seven species (w = 3.91248).

3.2.2. Large communities

As in the unimodal case, after analyzing the initial bifurcations, we extend the bifurcation diagram to 25 species by increasing the range of resources and investigate the emerging trait patterns (Fig. 7). The increased diversity is generated by the two types of bifurcations we characterized in the previous section, which alternate to add species to the ESC as the resource distribution becomes wider. The impact of competition on the trait structure is modulated by the bimodality of the intrinsic growth function, but only at low widths of the growth function, where competition results in evenly spaced traits centered on the two peaks in the intrinsic growth function. At high widths however, competition is more localized in trait space and the species at ESC become evenly distributed across the entire width.

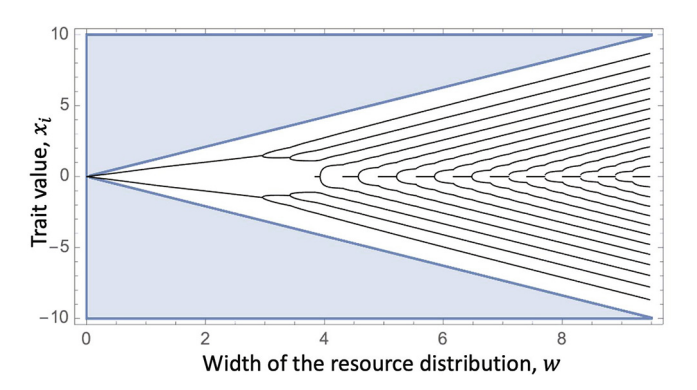


Fig. 7. The trait patterns of communities up to 25 species as the width of the bimodal intrinsic growth function is increased. At low widths, competition results in evenly spaced species corresponding to each peak of the bimodal growth function. However, with increased widths, species can grow with traits corresponding to the minima of the bimodal growth function. Therefore, competition results in equal spacing of the traits across the entire trait axis where the intrinsic growth rate of the species is positive.

3.3. Comparison of the unimodal and bimodal cases

Here, we compare the patterns of community structure generated under the two intrinsic growth functions (unimodal and bimodal). Since the competition kernel is common between the two scenarios, comparing them allows us to understand the role of the shape of the resource distribution. In this section, we compare both the trait patterns from the bifurcation diagrams discussed above. Further, we also calculate the total competition faced by the species at ESC under both intrinsic growth functions and compare it to the intrinsic growth function.

In both cases, we found that increasing the width of the resource distribution results in greater diversity (Figs. 4 and 7). This is intuitive because wide resource distributions mean that species can evolve to consume different types of resources, thus reducing interspecific competition and allowing more species to coexist. In contrast, narrow resource distributions restrict the species to a limited resource range, which increases competition between the species most adapted to the dominant resource and others. This competition consequently leads to the extinction of any species not adapted to the dominant resource, reducing diversity.

The trait patterns in the unimodal and bimodal cases also make for an interesting comparison. For low w, the number of species in the bimodal resource distribution ESCs (Fig. 7) is twice the number of species in the unimodal resource distribution ESCs (Fig. 4). This is a direct result of the underlying resource distribution allowing two different dominant resources, which results in species evolving towards traits which allow for optimal consumption of these resources. However, as w becomes larger, the diversity generated in the bimodal case becomes equal to the diversity generated in the unimodal case. In large communities, diversity is proportional to the width of the resource distribution. Wider resource distributions allow more species, which leads to more localized competition and slightly tighter packing of species in trait space. Even species with the lowest intrinsic growth rates (corresponding to the minimum of the growth function) are part of the ESC, thus erasing the effect of the shape of resource distribution on the resultant trait patterns altogether.

While the role of the shape of the resource distribution on the community cannot be seen through the trait distribution at high w, the competition faced by the species at ESC is clearly shaped by the underlying resource distributions. In Fig. 8, the competitive impact on growth rate by each species, $\alpha(x,x_i)\hat{n}_i$, at a 20-species ESC is shown by the series of smaller curves in each panel. Since the competitive impacts are weighted by abundance, which is directly linked to the intrinsic growth rate (Fig. 8a, b), the intrinsic growth rate functions determine the total competitive impact from all the species at ESC, $\sum_{j=1}^{N} \alpha(x, x_j) \widehat{n}_j$. This can be shown by the taller curves in Fig. 8c and d, where the total competitive impact is very close to the intrinsic growth rate for traits where the intrinsic growth rate is positive. For the species in the ESC, the total competitive impact is nearly identical to the intrinsic growth rate. However, since the difference between the intrinsic growth rate and the total competitive trait is extremely small for the remaining trait values, the curves look virtually identical in the figures except beyond the range of the community.

The underlying explanation for the close match between the total competitive impact and the intrinsic growth function is that the equilibrium abundance \widehat{n}_j of the species j is more or less proportional to the intrinsic growth rate (Fig. 8a, b). Since this holds true for both shapes of the intrinsic growth curve, the match between the total competitive impact and intrinsic growth also holds for both shapes of the intrinsic growth function (Fig. 8c, d). Therefore, this observation is independent of the shape of the intrinsic growth function and unifies both the cases.

3.4. What does competitive coevolution maximize?

The close match between the intrinsic growth rate function and the total competition exerted by the community in Fig. 8 suggests that the trait-based eco-evolutionary community assembly process acts to maximize the use of available resources. In a purely ecological context, MacArthur (1969, 1970) found a quantity that is minimized by equilibrium population sizes \hat{n}_i in symmetric Lotka-Volterra competition. In a lesser-known paper, Matessi and Jayakar (1981) extended this result to an eco-evolutionary setting with a fixed number of species. Specifically, they derived two quantities that are maximized by coevolution; in terms of our parameterization, they are:

$$\Psi(\vec{\mathbf{x}}, \vec{\mathbf{n}}) = \sum_{i=1}^{\mathcal{N}} \left(2r(\widehat{\mathbf{x}}_i) - \sum_{j=1}^{\mathcal{N}} \alpha(\widehat{\mathbf{x}}_i, \widehat{\mathbf{x}}_j) \widehat{\mathbf{n}}_j \right) \widehat{\mathbf{n}}_i$$

and

$$\Gamma\left(\overrightarrow{x}\right) = \left(\sum_{i=1}^{\mathscr{N}} r(\widehat{x}_i) \, \widehat{n}_i\right)^2 / \sum_{j=1}^{\mathscr{N}} \alpha(\widehat{x}_i, \widehat{x}_j) \, \widehat{n}_i \, \widehat{n}_j$$

The difference between them is that ψ maximized over both the traits \overrightarrow{x} and the population sizes \overrightarrow{n} , whereas Γ is maximized only over the traits, with the population sizes taken as functions of the trait values. Note that these extremum principles apply only to the case of symmetric competition, where $\alpha(x,y) = \alpha(y,x)$.

We found that these functions are also applicable to our ecoevolutionary LV model with a variable number of species \mathcal{N} . Fig. 9 plots Γ as a function of trait values, superimposed on a mutual invasibility plot (MIP), which shows sets of species that can coexist (Geritz et al. 1998), for a range of resource distribution widths corresponding to one- to four-species ESCs in the unimodal case. The dots correspond to the ESCs found in our bifurcation diagram (Fig. 4). Fig. 9A-B are standard MIPs with the traits of two species on the axes. To show that Γ is also maximized in more diverse communities, Fig. 9C-F are non-standard MIPs that assume the symmetry found in Fig. 4, which allows us to illustrate up to

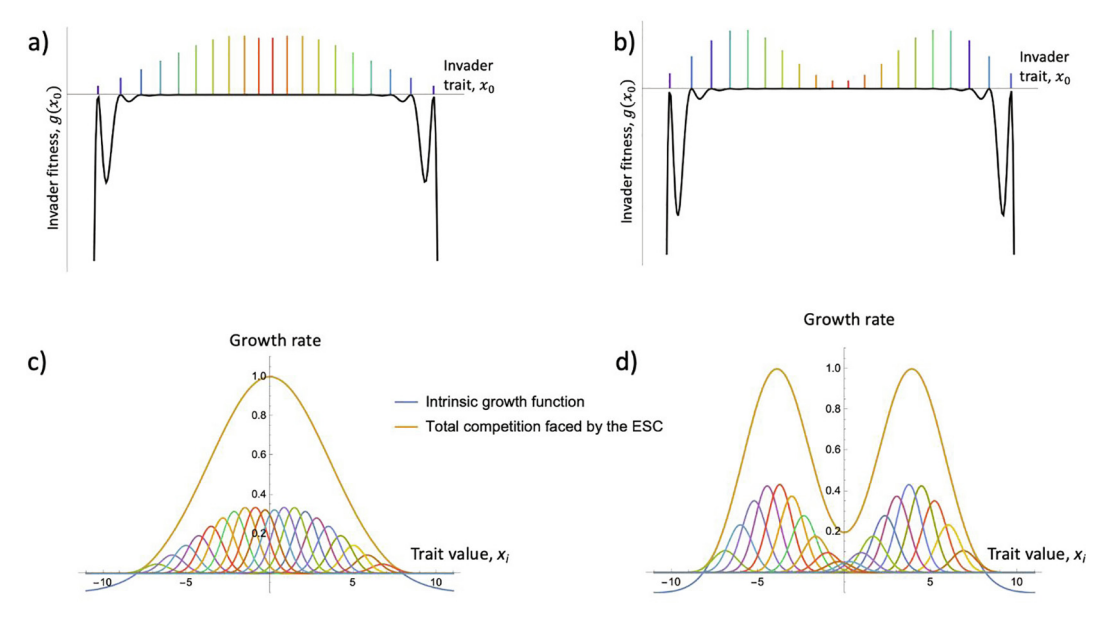


Fig. 8. The impact of the intrinsic growth rate function on the (a, b) abundance and the (c, d) total competition faced by species in a 20-species ESC. The 20-species ESC is shown under both shapes of the intrinsic growth function - (a, c) unimodal and (b, d) bimodal. The panels in the top row (a, b) show the invasion fitness landscape (the black curve) of a 20-species ESC under the (a) unimodal and (b) bimodal intrinsic growth function. The traits of resident species at ESC are denoted by the vertical bars and their abundances are proportional to the height of the bars. As can be seen in both (a) and (b), the abundances of the species at ESC are largely determined by the intrinsic growth function. The panels in the bottom row (c, d) compare the total competition faced by 20 species ESC in the (a) unimodal and (b) bimodal cases to the intrinsic growth rate. The abscissa represents the trait values and the ordinate is in units of growth rate. The blue curves in (c) and (d) denote the unimodal and bimodal intrinsic growth functions respectively. The series of smaller curves in both panels show the amount of competition each species at the ESC faces from species with trait value x_i . Finally, the tall yellow curve in (c) and (d) shows the sum of the competitive impacts of a species with trait x_i on the 20 species in ESC. As can be seen, the total competition faced by the ESC follows the shape of the intrinsic growth rate function closely. (For interpretation of the references to colour in this figure legend, the reader is referred to the web version of this article.)

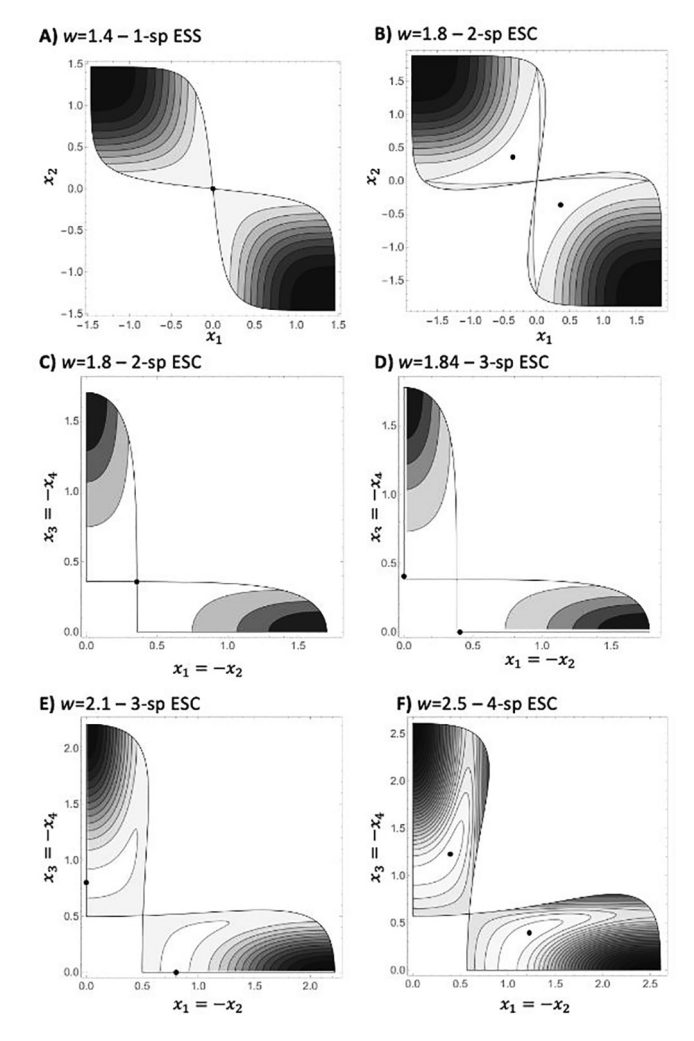


Fig. 9. Γ as a function of trait values for different values of the resource distribution width w. Shaded regions indicate sets of species that can mutually invade (MIPs), and lighter colors correspond to higher values of Γ . Dots indicate ESCs extracted from our bifurcation diagram (Fig. 4). **A-B**) are traditional MIPs, with up to two species. **C-F**) assume symmetry to show up to four species.

four species in a two-dimensional plot. In all cases, the ESCs can be seen to maximize Γ , which we verified numerically.

While the Γ function is maximised over traits, it also allows us to interpret the number of species present at ESC. Specifically, when maximization of the Γ function is done in more dimensions than the number of species present at ESC, the resulting maximum always shows redundant species. In Fig. 9A, the maximization is done in two dimensions but the ESC lies at $x_1 = x_2 = 0$, thus showing a redundant second species. Similarly, in Fig. 9C, the maximization is done in four dimensions but the ESC lies on the diagonal of the plot such that there are only two distinct trait values at ESC. In Fig. 9D-E, the maximization is again done in four dimensions but the ESC lies on the edge of the plot resulting in only three distinct trait values.

4. Discussion

The LV model has a long history for studying competition, but studies of diversification have not mapped out the effect of parameters such as the width of the intrinsic growth function beyond two-or three-species communities in a continuous fashion. Moreover, the role of changing underlying resource distributions on the outcome of these diversification processes remains unclear. We address both of these questions using a trait-based LV competition model, where we analyze the how community structure depends on the

shape and width of the underlying intrinsic growth rate function. We choose two different shapes —unimodal and bimodal — to mimic resource distributions in nature where one or two resource types are prominent. These resource distributions are modeled implicitly through trait-dependent intrinsic growth functions.

In the unimodal model, the traits at the ESC are roughly evenly spaced over the trait axis, displaying limiting similarity. Even in the bimodal model, the resulting traits become approximately evenly distributed at large w, within the constraints set by the resource distribution. Such patterns have previously been seen in LV models (MacArthur and Levins, 1967), in spatial models (Mágori et al., 2005; Pontarp et al., 2015), seasonal models (Kremer et al., 2017) and models with environmental stochasticity (May 1973; May & MacArthur, 1972). However, none of these previous studies examined these patterns for more than three species under continuously varying width of the environment except Kremer et al., 2017 (but see examples of large communities at a fixed widths in Bonsall et al., 2004; Cressman et al., 2017; Hui et al., 2018). We have examined this pattern for up to 25 species in both environments and find that the pattern is robust.

We also investigated the impact of the width of the resource distributions on community structure in these models. In general, wider resource distributions resulted in higher diversity. Narrow resource distributions results constrain the fundamental niche of the species, resulting in lower diversity. As the resource distributions become wider, more resources become available to the competitors, which allows for higher diversity. This process is modulated by the shape of the resource distribution. At narrow widths in the bimodal case, competition resulted in twice the diversity observed in the unimodal case. However, as the width of the distribution increases, competition becomes more localized and the resulting diversity patterns become similar under both growth functions

The resulting diversity under both growth functions was generated via two types of bifurcations — one involving the loss of local evolutionary stability of one of the species in the ESC and another involving the loss of global stability of the ESC. For unimodal resource distributions (and practically for bimodal resource distributions, see Fig. 5), these bifurcations alternate in transitions to higher numbers of species. While ESCs just past the bifurcation involving the loss of local stability can be attained by following adaptive dynamics methods, the focus of adaptive dynamics on invaders with small trait differences from the resident means that the loss of global stability does not immediately lead to increased diversity. Interestingly, as can be seen in the bifurcation from two to four species in the bimodal case (Fig. 5), local evolutionary stability is typically lost for slightly larger widths after loss of global stability.

The shape of the growth functions helps us draw insights about the interplay of competition with the environment to generate patterns of trait distribution in communities. While the traits of the species were roughly evenly spaced under both growth functions, they were evenly spaced within the two peaks of the bimodal fundamental growth rate function at narrow widths. Therefore, competition acts to evenly space traits within the constraints set by the environment. However, this distinction vanishes when the resource distributions become extremely large. Large w leads to similar trait patterns in both unimodal and bimodal environments. This shows that when the resource distributions are extremely wide, traits become evenly spaced irrespective of the environmental filter.

A clearer picture of the role of the growth function emerges from the competition generated by the species (Fig. 8). While the trait patterns are overwhelmingly determined by competition, the competition these species face is clearly linked to resource availability. The abundance of the species is determined by the resources available for it to consume, which in turn determines

the competitive impact it generates. Therefore, the sum of the competitive impacts faced by each species at ESC is unimodal when the growth function is unimodal and demonstrates a clear bimodality under a bimodal growth function. Therefore, while making inferences from trait patterns about the processes acting in the community, it is critical to include competitive impacts on the species in the community. Since the equilibrium abundances are more or less proportional to the resource availability, measuring abundances in conjunction with the traits empirically is a feasible, albeit not fully accurate alternative to measuring competition strengths.

As in previous symmetrical ecological (Mac Arthur, 1969; MacArthur, 1970) and eco-evolutionary LV models (Matessi and Jayakar, 1981), we find that the ESC maximizes a function that describes the match between resource supply and utilization (Fig. 9). This maximization principle might provide a viable alternative numerical method for finding ESCs, but it is currently limited to symmetric LV models (but see Marsland et al., 2020 for an extension to a range of resource competition models). Its real utility is in illuminating how competition acts to best match the resource distribution provided by the environment.

More broadly, our results confirm and contribute towards a fairly general understanding of limiting similarity (Abrams, 1983; MacArthur and Levins, 1967). The number of species at ESC is proportional to the width of the fundamental community (trait space where r(x) > 0) divided by the spacing between species (Barabás et al., 2016; Barabás and Meszéna, 2009; Kremer et al., 2017; MacArthur and Levins, 1967; Scheffer and van Nes, 2006; Szabó and Meszéna, 2006). Therefore, the number of potential species at ESC scales directly with the width of the fundamental community. This allows us to predict the diversity and structure of communities without having to identify the ESC itself. Further, since this scaling holds true across different shapes of the intrinsic growth function, the precise shape of the intrinsic growth function ceases to be significant for the prediction of community structure particularly for large communities. This holds true as long as the intrinsic growth function is positive in a well-defined compact region and zero or negative outside it.

In a review on linking trait patterns to niche differentiation, D'Andrea and Ostling (2016) call for more simple conceptual models exploring various biological complexities. In this work, we have taken a step in that direction by exploring a simple model incorporating both evolution and different environments. We have shown that competition can lead to diverse communities, if the width of the resource distribution is large. We have also shown that while the resulting trait patterns contain signatures of the environment, they are ultimately driven by competition. Future empirical work using trait patterns to characterize processes like competition needs to consider the role of the width of the resource distribution of the competing species.

CRediT authorship contribution statement

Ravi Ranjan: Formal analysis, Methodology, Writing – original draft, Writing – review & editing, Visualization. **Christopher A. Klausmeier:** Conceptualization, Methodology, Software, Writing – review & editing, Resources, Supervision, Funding acquisition.

Declaration of Competing Interest

The authors declare that they have no known competing financial interests or personal relationships that could have appeared to influence the work reported in this paper.

Acknowledgments

We would like to thank Meredith Zettlemoyer, Thomas Koffel, Jonas Wickman and other members of the Litchman-Klausmeier lab for comments. We would also like to thank György Barabás and another anonymous reviewer for feedback which improved this manuscript substantially. This research was supported by a grant from the Simons Foundation, United States (Award Number 343149) to C.A.K & E. Litchman. This is Kellogg Biological Station contribution number 2310.

References

- Abrams, P., 1983. The theory of limiting similarity. Annu. Rev. Ecol. Syst. 14, 359–376. https://doi.org/10.1146/annurev.es.14.110183.002043.
- Ackermann, M., Doebeli, M., 2004. Evolution of niche width and adaptive diversification. Evolution 58, 2599–2612.
- Barabás, G., Pigolotti, S., Gyllenberg, M., Dieckmann, U., Meszéna, G., 2012. Continuous coexistence or discrete species? A new review of an old question. Evol. Ecol. Res. 14, 523–554.
- Barabás, G., Meszéna, G., 2009. When the exception becomes the rule: The disappearance of limiting similarity in the Lotka-Volterra model. J. Theor. Biol. 258, 89–94. https://doi.org/10.1016/j.jtbi.2008.12.033.
- Barabás, G., D'Andrea, R., Vasseur, D., 2016. The effect of intraspecific variation and heritability on community pattern and robustness. Ecol. Lett. 19, 977–986. https://doi.org/10.1111/ele.12636.
- Birand, A., Barany, E., 2014. Evolutionary dynamics through multispecies competition. Theor. Ecol. 7, 367–379. https://doi.org/10.1007/s12080-014-0224-x.
- Bonsall, M.B., Jansen, V.A.A., Hassell, M.P., 2004. Life history trade-offs assemble ecological guilds. Science 306, 111–114. https://doi.org/10.1126/science.1100680.Brown, J.S., Vincent, T.L., 1987. A theory for the evolutionary game. Theor. Popul. Biol. 31, 140–166.
- Connell, J.H., 1983. On the prevalence and relative importance of interspecific competition: evidence from field experiments. Am. Nat. 122, 661–696.
- Cressman, R., Halloway, A., McNickle, G.G., Apaloo, J., Brown, J.S., Vincent, T.L., 2017. Unlimited niche packing in a Lotka-Volterra competition game. Theor. Popul. Biol. 116, 1–17. https://doi.org/10.1016/j.tpb.2017.04.003.
- D'Andrea, R., Ostling, A., 2016. Challenges in linking trait patterns to niche differentiation. Oikos 125, 1369–1385. https://doi.org/10.1111/oik.02979.
- Della Rossa, F., Dercole, F., Landi, P., 2015. The branching bifurcation of adaptive dynamics. Int. J. Bifurc. Chaos 25, 1540001. https://doi.org/10.1142/ S0218127415400015
- Dercole, F., Geritz, S.A.H., 2016. Unfolding the resident–invader dynamics of similar strategies. J. Theor. Biol. 394, 231–254. https://doi.org/10.1016/j.itbi.2015.11.032.
- Dercole, F., Della Rossa, F., Landi, P., 2016. The transition from evolutionary stability to branching: a catastrophic evolutionary shift. Sci. Rep. 6, 26310. https://doi.org/10.1038/srep26310.
- Edwards, K.F., Kremer, C.T., Miller, E.T., Osmond, M.M., Litchman, E., Klausmeier, C. A., Becks, L., 2018. Evolutionarily stable communities: a framework for understanding the role of trait evolution in the maintenance of diversity. Ecol. Lett. 21, 1853–1868. https://doi.org/10.1111/ele.13142.
- Elton, C., 1946. Competition and the structure of ecological communities. J. Anim. Ecol. 15, 54. https://doi.org/10.2307/1625.
- Fort, H., Scheffer, M., van Nes, E.H., 2009. The paradox of the clumps mathematically explained. Theor. Ecol. 2, 171–176. https://doi.org/10.1007/s12080-009-0040-x.
- Gallien, L., Landi, P., Hui, C., Richardson, D.M., Allan, E., 2018. Emergence of weak-intransitive competition through adaptive diversification and eco-evolutionary feedbacks. J. Ecol. 106, 877–889. https://doi.org/10.1111/1365-2745.12961.
- Geritz, S.A.H., Kisdi, E., Meszena, G., Metz, J.a.J., 1998. Evolutionarily singular strategies and the adaptive growth and branching of the evolutionary tree. Evol. Ecol. 12, 35–57. https://doi.org/10.1023/A:1006554906681.
- Geritz, S.A.H., van der Meijden, E., Metz, J.A.J., 1999. Evolutionary dynamics of seed size and seedling competitive ability. Theor. Popul. Biol. 55, 324–343. https://doi.org/10.1006/tpbi.1998.1409.
- Hui, C., Richardson, D.M., Landi, P., Minoarivelo, H.O., Garnas, J., Roy, H.E., 2016. Defining invasiveness and invasibility in ecological networks. Biol. Invasions 18, 971–983. https://doi.org/10.1007/s10530-016-1076-7.
- Hui, C., Minoarivelo, H.O., Landi, P., 2018. Modelling coevolution in ecological networks with adaptive dynamics. Math. Methods Appl. Sci. 41, 8407–8422. https://doi.org/10.1002/mma.4612.
- Hui, C., Richardson, D.M., Landi, P., Minoarivelo, H.O., Roy, H.E., Latombe, G., Jing, X., CaraDonna, P.J., Gravel, D., Beckage, B., Molofsky, J., 2021. Trait positions for elevated invasiveness in adaptive ecological networks. Biol. Invasions 23, 1965– 1985. https://doi.org/10.1007/s10530-021-02484-w.
- Kisdi, É., 1999. Evolutionary branching under asymmetric competition. J. Theor. Biol. 197, 149–162.
- Klausmeier, C.A., Kremer, C.T., Koffel, T., 2020. Trait-based ecological and eco-evolutionary theory. In: McCann, K.S., Gellner, G. (Eds.), Theoretical Ecology. Oxford University Press, pp. 161–194. https://doi.org/10.1093/oso/9780198824282.003.0011.

- Klausmeier, C.A., 2020. EcoEvo v 1.6.3. https://github.com/cklausme/EcoEvo/.
- Kremer, C.T., Klausmeier, C.A., Grover, J., 2017. Species packing in eco-evolutionary models of seasonally fluctuating environments. Ecol. Lett. 20, 1158–1168. https://doi.org/10.1111/ele.12813.
- Kuno, E., 1991. Some strange properties of the logistic equation defined with r and K: inherent defects or artifacts? Res. Popul. Ecol. 33, 33–39. https://doi.org/ 10.1007/BF02514572.
- Landi, P., Dercole, F., Rinaldi, S., 2013. Branching scenarios in eco-evolutionary preypredator models. SIAM J. Appl. Math. 73, 1634–1658. https://doi.org/10.1137/ 12088673Y
- Lotka, A.J., 1925. Elements of physical biology. Williams and Wilkins Co..
- Mac Arthur, R.M., 1969. Species packing, and what competition minimizes. Proc. Natl. Acad. Sci. 64, 1369–1371.
- MacArthur, R., 1970. Species packing and competitive equilibrium for many species. Theor. Popul. Biol. 1, 1–11. https://doi.org/10.1016/0040-5809(70)90039-0.
- MacArthur, R.H., 1972. Geographical ecology: patterns in the distribution of species. Princeton University Press.
- Macarthur, R., Levins, R., 1967. The limiting similarity, convergence, and divergence of coexisting species. Am. Nat. 101, 377–385.
- Mágori, K., Szabó, P., Mizera, F., Meszéna, G., 2005. Adaptive dynamics on a lattice: role of spatiality in competition, co-existence and evolutionary branching. Evol. Ecol. Res. 7, 1–21.
- Mallet, J., 2012. The struggle for existence: how the notion of carrying capacity, K, obscures the links between demography, Darwinian evolution, and speciation. Evol. Ecol. Res. 14, 627–665.
- Marsland, R., Cui, W., Mehta, P., 2020. The minimum environmental perturbation principle: a new perspective on niche theory. Am. Nat. 196, 291–305. https:// doi.org/10.1086/710093.
- Matessi, C., Jayakar, S.D., 1980. Models of density- and frequency- dependent selection for the exploitation of resources. II. Coevolution of species in competition. In: Barigozzi, C. (Ed.), Vito Volterra Symposium on Mathematical Models in Biology., Lecture Notes in Biomathematics. Springer, Berlin Heidelberg, p. 18.
- Matessi, C., Jayakar, S.D., 1981. Coevolution of species in competition: a theoretical study. Proc. Natl. Acad. Sci. 78, 1081–1084.
- May, R.M., 1973. Stability and Complexity in Model Ecosystems. Princeton University Press, Princeton.

- May, R.M., Arthur, R.H.M., 1972. Niche overlap as a function of environmental variability. Proc. Natl. Acad. Sci. 69, 1109–1113.
- Mcgill, B., Enquist, B., Weiher, E., Westoby, M., 2006. Rebuilding community ecology from functional traits. Trends Ecol. Evol. 21, 178–185. https://doi.org/10.1016/j. tree.2006.02.002.
- Messier, J., McGill, B.J., Lechowicz, M.J., 2010. How do traits vary across ecological scales? A case for trait-based ecology. Ecol. Lett. 13, 838–848. https://doi.org/10.1111/j.1461-0248.2010.01476.x.
- Metz, J.A.J., Geritz, S.A.H., Meszéna, G., Jacobs, F.J.A., van Heerwarden, J.S., 1996. Adaptive dynamics: a geometrical study of the consequences of nearly faithful reproduction Amsterdam: North Holland. In: van Strien, S.J., Verduyn Lunel, S. M. (Eds.), Stochastic and Spatial Structures of Dynamical Systems, pp. 183–231.
- Minoarivelo, H.O., Hui, C., 2016. Invading a mutualistic network: to be or not to be similar. Ecol. Evol. 6, 4981–4996. https://doi.org/10.1002/ece3.2263.
- Pastore, A.I., Barabás, G., Bimler, M.D., Mayfield, M.M., Miller, T.E., 2021. The evolution of niche overlap and competitive differences. Nat. Ecol. Evol. 5, 330–337. https://doi.org/10.1038/s41559-020-01383-y.
- Polechová, J., Barton, N.H., 2005. Speciation through competition: a critical review. Evolution 59, 1194–1210. https://doi.org/10.1111/j.0014-3820.2005.tb01771.x.
- Pontarp, M., Ripa, J., Lundberg, P., 2015. The biogeography of adaptive radiations and the geographic overlap of sister species. Am. Nat. 186, 565–581. https://doi.org/10.1086/683260.
- Priklopil, T., 2012. On invasion boundaries and the unprotected coexistence of two strategies. J. Math. Biol. 64, 1137–1156. https://doi.org/10.1007/s00285-011-0448-v.
- Roughgarden, J., 1979. Theory of population genetics and evolutionary ecology: an introduction.
- Scheffer, M., van Nes, E.H., 2006. Self-organized similarity, the evolutionary emergence of groups of similar species. Proc. Natl. Acad. Sci. 103, 6230–6235. https://doi.org/10.1073/pnas.0508024103.
- Szabó, P., Meszéna, G., 2006. Limiting similarity revisited. Oikos 112, 612–619. https://doi.org/10.1111/j.0030-1299.2006.14128.x.
- Volterra, V., 1926. Fluctuations in the abundance of a species considered mathematically. Nature 2972, 558–560.
- Wolfram Research, Inc., 2021. Mathematica. Champaign, Illinois. https://www.wolfram.com/mathematica.